Available online at www.sciencedirect.com
ScienceDirect
Journal of the European Ceramic Society 30 (2010) 999–1005
www.elsevier.com/locate/jeurceramsoc

Microstructure of boron carbide pressureless sintered in an Ar atmosphere containing gaseous metal species

Hiroyuki Miyazaki [a,*], You Zhou [a], Hideki Hyuga [a], Yu-ichi Yoshizawa [a], Takeshi Kumazawa [b]

[a] *National Institute of Advanced Industrial Science and Technology (AIST), Anagahora 2266-98, Shimo-shidami, Moriyama-ku, Nagoya 463-8560, Japan*
[b] *Mino Ceramic CO., LTD., 1-46, Kamezaki Kitaura-cho, Handa-shi, Aichi prefecture 475-0027, Japan*

Received 20 April 2009; received in revised form 2 October 2009; accepted 20 October 2009

Abstract

97.4% of theoretical density was obtained for boron carbide (B_4C) ceramics by heating up to 2226 °C in an Ar atmosphere containing gaseous Al and Si species without external pressure. Impurities and secondary phases in the sintered B_4C samples were examined by X-ray fluorescence and X-ray diffraction analyses respectively, which revealed that both Al and Si elements infiltrated into the green compacts and reacted with B_4C to form SiC, Al_4C_3 and Al_4SiC_4 during the sintering. Triple junctions observed in the polished surfaces of the densified samples were filled by the secondary phases, indicating formation of liquid phase during heating. Dilatometric measurements at a constant heating rate in the Ar gas with the metallic gas species demonstrated that the shrinkage started at around 1700 °C, which was the liquid-phase formation temperature for the system reported in the previous studies. It was supposed that the liquid phase might be responsible for the densification.

Keywords: Sintering; Microstructure-final; Carbide; Boron carbide

1. Introduction

Thanks to its high hardness, high Young's modulus and low theoretical density boron carbide (B_4C) is a candidate material for such structural components especially where high specific elastic modulus and/or hardness are required.[1] However, pressureless sintering of B_4C is difficult due to the strong covalent bonding of B–C. Many researchers have tried to sinter B_4C at ambient pressure by adding sintering aids such as C,[2–4] Al_2O_3[5] TiC[6] and TiB_2.[7] In these reports, full densification was attained with a lot of sintering additives although the superior characteristics of B_4C was not fully developed owing to the presence of many secondary phases. Heating in a He-H_2 atmosphere[8] or rapid heating[9] are the alternatives to the sintering additives, both of which are unsuitable for industrial applications. Hot pressing was another route to produce dense B_4C products, but their shapes are limited to only simple ones or much cost is needed to machine complex parts. Thus, B_4C ceramics has been only used for the special applications such as sand blast nozzles, etc.

In our previous study, B_4C was densified up to 97.4% of theoretical density at 2226 °C by employing an Ar atmosphere containing gaseous metal species under an ambient pressure.[10] In this study, green compacts with different densities were sintered under the same condition as previous study. Impurities and crystalline phases in the densified samples were identified using both X-ray fluorescence and X-ray diffraction (XRD) analyses and their microstructures were observed with scanning electron microscopy (SEM) and energy dispersive X-ray spectroscopy (EDS). Sintering behavior of the compact was monitored using a dilatometer up to 2050 °C at a constant heating speed. The mechanism of pressureless sintering of B_4C is discussed in conjunction with the effect of green density on the microstructure.

2. Experimental procedures

High-purity B_4C powder with a specific surface area of 18 m^2/g (grade HS, H.C. Starck GmbH & Co., Berlin, Germany) was used as a starting powder. The powder contains minor amounts of graphite and boron oxide.[10] Other impurities and distribution of particle size were presented in our previous paper.[10] Pellets of Ø 25 mm × 5 mm were prepared by pressing the raw powder uniaxially at 9.8 MPa, followed by cold isostatic press-

* Corresponding author. Tel.: +81 52 736 7486; fax: +81 52 736 7405.
E-mail address: h-miyazaki@aist.go.jp (H. Miyazaki).

0955-2219/$ – see front matter © 2009 Elsevier Ltd. All rights reserved.
doi:10.1016/j.jeurceramsoc.2009.10.015

ing (CIP) at 490 MPa. In order to study effects of green density on bulk density, several pellets were CIPed at 98 MPa. The relative density of the compacts CIPed at 490 MPa was 70.0%, whereas that of ones CIPed at 98 MPa was 65.7%. The green compacts were set in a graphite crucible together with powder mixture of SiC (grade OY-15, Yakushima Denko, Tokyo, Japan) and aluminum (reagent grade, Soekawa Chemical Co. Ltd., Tokyo, Japan). The weight of the powder mixture was about 3 g and the mass ratio of SiC to Al powders was 30:1. The powder was spread directly on the bottom of the crucible, while the compacts were put on a carbon block separately from the powder. The graphite resistance furnace (Chugai Ro, Co. Ltd., Osaka, Japan) was employed to sinter the samples up to 2226 °C at a heating rate of 10 °C/min. At first step, the compacts were heated from R.T. to 1900 °C in vacuum before introducing pure Ar gas to ambient pressure at 1900 °C for 10 min. Then the temperature was raised to each target temperature (2108–2226 °C). The soaking time for each target temperature was 4 h.

Density measurements were conducted using the Archimedes technique with distilled water. Relative densities were evaluated by using the theoretical density of B_4C of 2.52 g/cm^3. The sintered samples were ground with a diamond wheel followed by polishing with 3 μm and 0.5 μm diamond slurry to obtain mirror-finish surfaces. Chemical impurities were detected by X-ray fluorescence analysis (WDXRF, Model XRF-1500, Shimadzu Co., Kyoto, Japan). Rh was used as a target material to obtain intense X-ray irradiation. Acceleration voltage and electric current were 40 kV and 100 mA, respectively. The irradiation area on the sample surface was 20 mm in diameter. Secondary phases in the bulk samples were identified by X-ray diffraction using Cu Kα radiation (Model RINT 2500, Rigaku Co., Tokyo, Japan). The polished samples were etched in KIO_4-saturated phosphoric acid to reveal the grain boundaries.[2] The surfaces of samples were coated with a 30 nm thick layer of gold using a sputter coater (Model SC-701AY, Sanyou Electron Co. Ltd., Tokyo, Japan) before microstructural observations by field emission scanning electron microscopy (Model JSM-6330F, JEOL Ltd., Tokyo, Japan). Energy dispersive X-ray spectrometry (EDS, Model JED-2140, JEOL Ltd., Tokyo, Japan) at 15 keV was employed to analyze chemical compositions of the inclusions.

Dilatometric studies of the samples were performed under a constant heating rate of 6 °C/min in the crucible containing mixed powder of Al and SiC. The measurements were done with a self-made dilatometer using laser displacement meters (Model LB-080, Keyence Co., Osaka, Japan), which was equipped with the graphite resistance furnace (Tokyo Shinku Co., Tokyo, Japan). The temperature was increased up to 2050 °C, and then held for 15 min. The furnace was evacuated with the diffusion pump until ∼1730 °C, followed by inlet of Ar gas to ambient pressure. A pushrod was set vertically on the top surface of the green pellet whose height was ∼8 mm. The clearance between the pushrod and the hole in the cover of the crucible was tight so that the gaseous phase generated from the mixed powder during heating would not escape from the crucible. The movement of the pushrod was measured optically with a laser displacement detector with a resolution of 8 μm. The shrinkage of the compact during heating was attained by subtracting both theoretical thermal expansions of B_4C and elongations of the measuring system from the observed displacement of the pushrod.

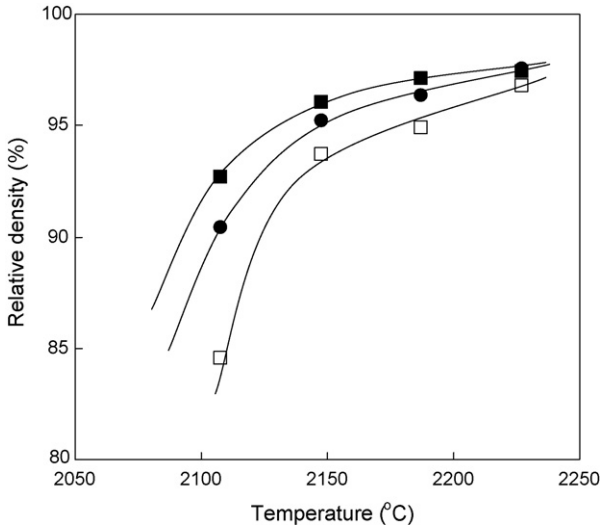

Fig. 1. Relative density versus sintering temperature for the pressurelessly sintered B_4C samples. Open marks represent the samples sintered in a pure Ar atmosphere, whereas closed ones correspond to samples sintered in the crucible containing powder mixture of Al and SiC in it. CIPing pressure for square and circle symbols were 490 MPa and 98 MPa, respectively.

3. Results

Fig. 1 shows the dependence of the relative densities of B_4C samples on the sintering temperature. The densities of the B_4C compacts CIPed at 490 MPa and sintered in the Ar atmosphere containing gaseous Si and Al species were larger than those of the compacts heated in the pure Ar gas at any sintering temperature and the maximum relative density of 97.4% was obtained at 2226 °C, whereas that of the sample sintered only in pure Ar gas was 96.8%. Densification of the compacts CIPed at 98 MPa and heated in the Ar atmosphere containing gaseous metal species was degraded slightly as compared with those of samples CIPed at 490 MPa when the temperature was below 2226 °C, which was attributable to the lower green density. But its maximum density at 2226 °C was almost identical to that of the sample with high green density. It should be noted that the relative densities of the compacts CIPed at 98 MPa were larger than those of samples CIPed at 490 MPa and sintered in the pure Ar gas especially at the relatively lower temperature ∼2100 °C irrespective to the lower green density.

Net peak intensities of X-ray fluorescence for metallic impurities in the three samples sintered at 2187 °C are presented in Fig. 2. Al was detected in both samples sintered together with the mixed powder of Al and SiC and its peak intensity in the sample CIPed at 98 MPa was much stronger than that of the sample CIPed at 490 MPa, while Al was hardly found in the sample sintered in the pure Ar atmosphere. The presence of Si in the sample sintered in the pure Ar gas was attributed to the impurity in the starting powder as described in the previous paper.[10] The amount of Si element in the samples heated together with the mixed powder of Al and SiC became larger than that in

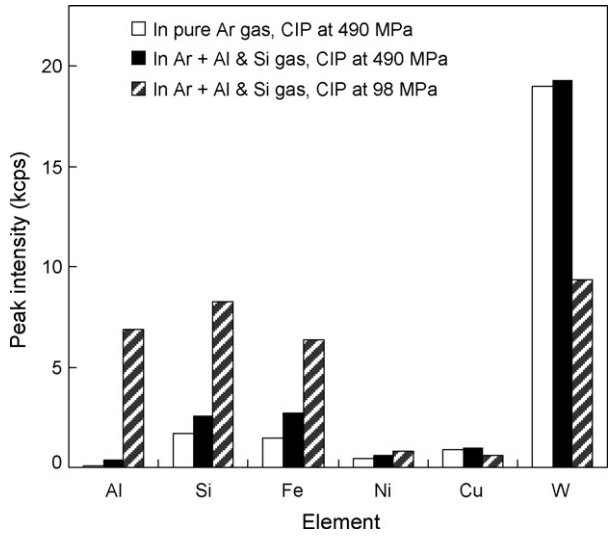

Fig. 2. Metallic impurities in the samples pressurelessly sintered at 2187 °C observed by X-ray fluorescence analysis.

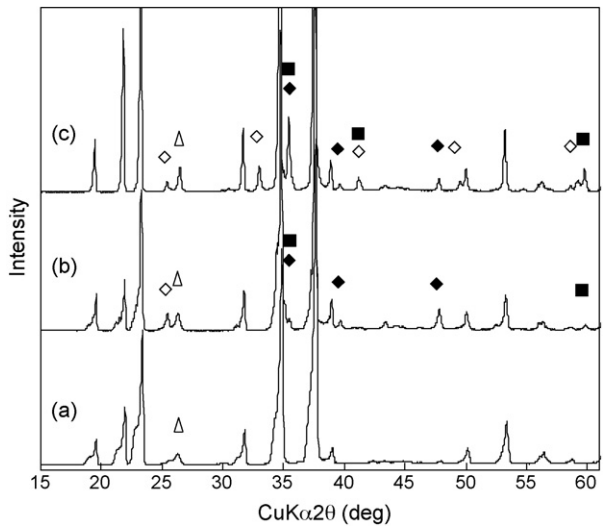

Fig. 3. X-ray diffraction patterns of the B_4C samples pressurelessly sintered at 2187 °C in (a) pure Ar gas (CIPed at 490 MPa), (b) Ar gas with metallic gaseous phase (CIPed at 490 MPa) and (c) Ar gas with metallic gaseous phase (CIPed at 98 MPa). △: graphite, ◇: Al_4SiC_4, ■: 3C-SiC, ♦: Al_4C_3.

the sample heated in the pure Ar gas. A significant increment in Si peak intensity was observed for the loose compact. The results suggested that metallic gas species were formed from the mixed powder of Al and SiC and penetrated into those compacts. Almost the same tendency was observed for the iron peaks as the Si peaks. The source of extra iron element in the samples sintered with the mixed powder may be the impurity in the Al and SiC powders, since the contents of iron impurity in the Al and SiC powders are 0.07 mass% and 0.01 mass%, respectively. The variations of both intensities for Ni and Cu were negligible, indicating that their origins were impurities in the starting B_4C powders. It is natural to infer that the notable intensity for W was due to its large atomic number ($Z = 74$) rather than its concentration since the fluorescence yield becomes larger as the atomic number increases. The origin of W was supposed to be the impurities in the B_4C starting powder, since the B_4C powders are usually obtained industrially by crushing B_4C ingots probably with WC.[1] The reason of the reduction in concentration for W observed in the densified sample using loose compact was not clear at this moment.

XRD charts of three samples sintered at 2187 °C with and without metallic gas species are presented in Fig. 3. Only a small amount of graphite was detected in the sample heated without sintering-aid gas, which came from the impurities in the raw powder (Fig. 3(a)).[10] By contrast, Al_4SiC_4, Al_4C_3 and 3C-SiC were identified besides the graphite phase in the samples sintered with the metallic gas species (Fig. 3(b), (c)). It is obvious that these phases in the samples were formed by the reaction of B_4C and/or carbon with both elements of Al and Si which diffused into the green compacts through vapor-phase transport. The peak intensity of Al_4SiC_4 and SiC in the sample whose CIP pressure was 98 MPa was larger than that in the sample CIPed at 490 MPa. It appeared that the amounts of secondary phases were abundant in the sample obtained from loose compact than that from dense one, which was consistent with the stronger peak intensities of X-ray fluorescence for Si and Al in the former sample than in the latter ones as described above.

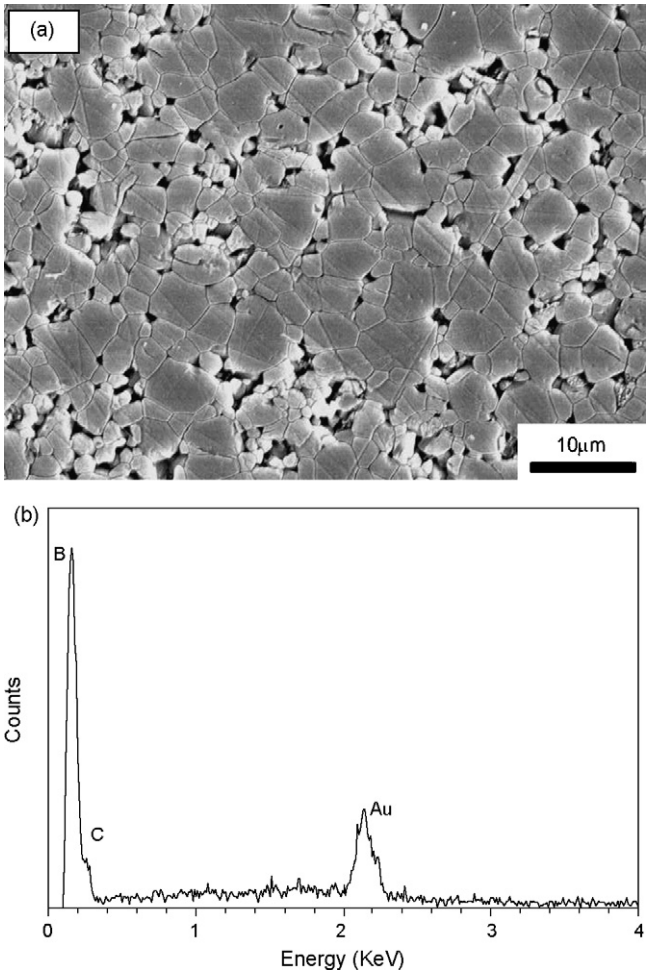

Fig. 4. (a) SEM image of the polished and etched surface of sample sintered at 2187 °C in pure Ar gas (CIPed at 490 MPa) and (b) EDS spectrum of whole area of the image.

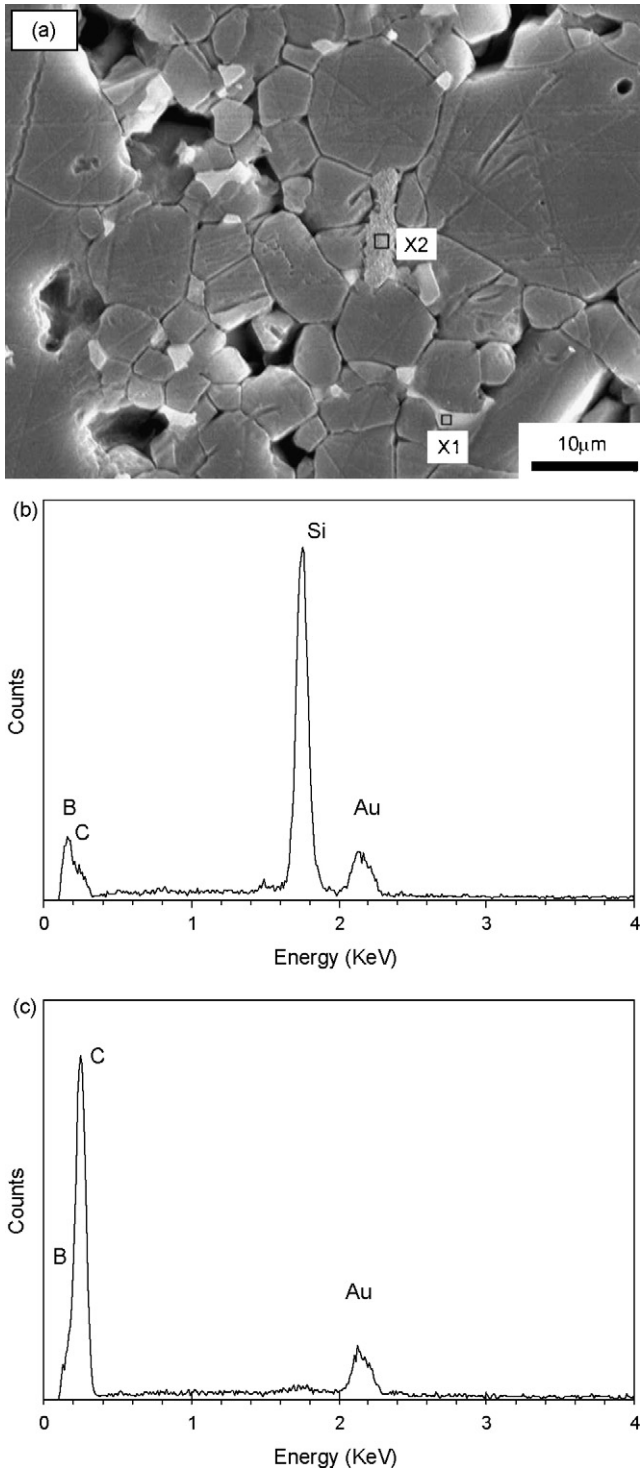

Fig. 5. (a) SEM image of the polished and etched surface of sample sintered at 2187 °C in Ar gas with metallic gaseous species (CIPed at 490 MPa) and EDS spectrum of (b) mark X1 and (c) mark X2.

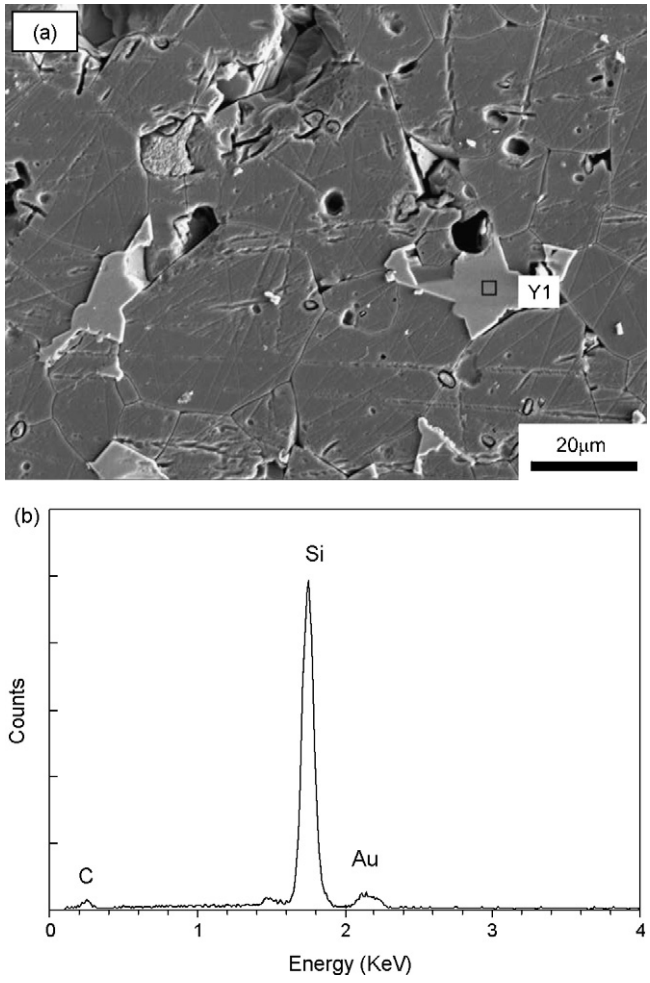

Fig. 6. (a) SEM image of the polished and etched surface of sample sintered at 2187 °C in Ar gas with metallic gaseous species (CIPed at 98 MPa) and (b) EDS spectrum of mark Y1.

In order to find the secondary phases identified by the XRD analysis, secondary electron microscopy equipped with EDS was performed for those samples heated at 2187 °C. SEM micrograph of the sample sintered in pure Ar gas revealed fine B_4C grains whose sizes were less than ~8 μm and many small residual pores with size less than ~2 μm (Fig. 4(a)). Secondary phases were hardly found in the SEM picture. EDS spectrum of the whole area of the micrograph did not show any peak of impurity other than Au which was derived from the Au coating for SEM observation (Fig. 4(b)).

In contrast, secondary phases whose morphologies were apparently different from that of the B_4C grains appeared in the micrograph of the sample obtained by sintering the dense compact in the Ar atmosphere with the sintering-aid gas (Fig. 5(a)). The bright secondary phases with irregular shapes were often observed at the triple junctions, indicating the presence of liquid phase during sintering at high temperature. EDS analysis on the spot in the bright secondary phase revealed that the main constituent element was Si (Fig. 5(b)). Based on the results of the XRD analysis, it was reasonably estimated that the candidate compound for this phase was SiC. Another type of secondary phase with rough surface was also observed in the middle of Fig. 5(a). The spectrum for the spot in the elongated grain exhibited a strong carbon peak (Fig. 5(c)), indicating that the graphite grains in the raw powder survived after sintering at high temperature, which is consistent with the results of XRD analysis. In Fig. 5(a), a few B_4C grains with size of ~20 μm were distributed among the major finer grains with size of 3–10 μm,

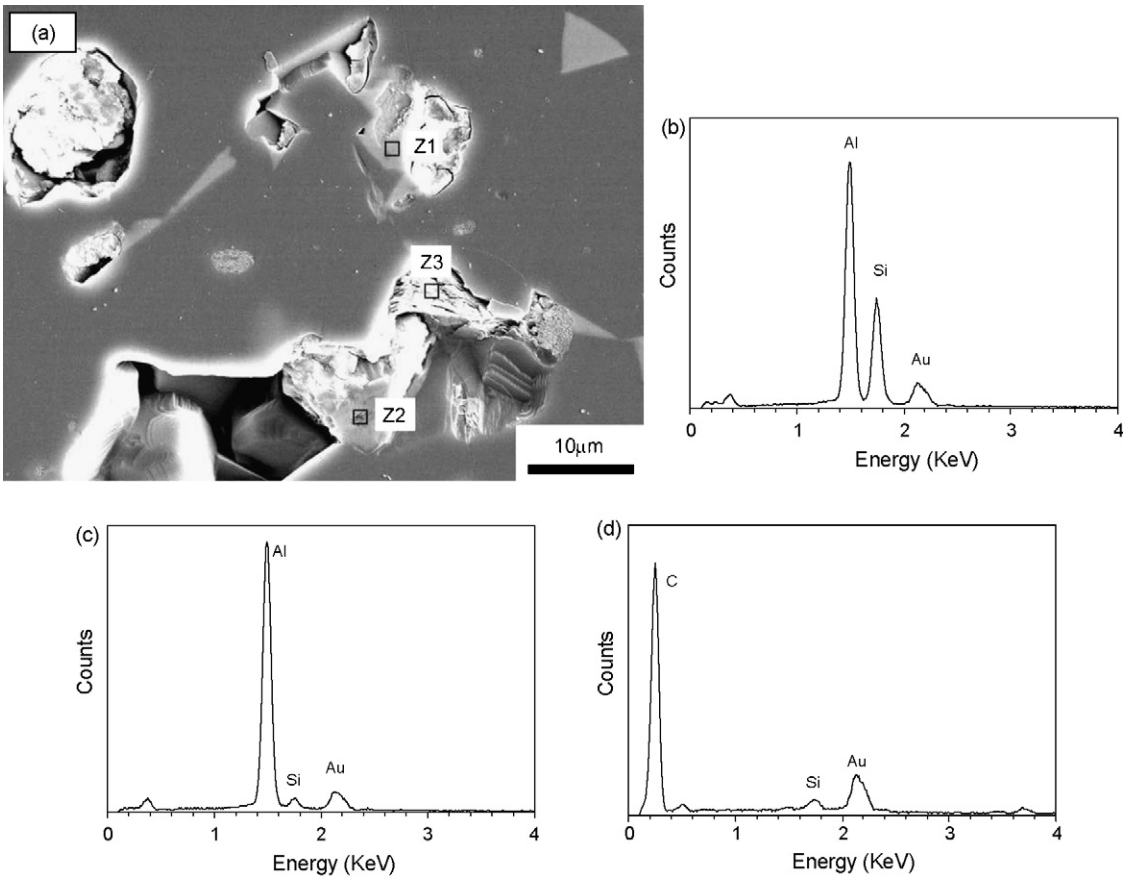

Fig. 7. (a) SEM image of sample sintered at 2187 °C in Ar gas with metallic gaseous species (CIPed at 98 MPa) and EDS spectrum of (b) mark Z1, (c) mark Z2 and (d) mark Z3. The surface was not etched after polishing to preserve unstable phases from disolution.

indicating that the exaggerated grain growth of B_4C took place.

In the case of the sample obtained by sintering the loose compact in the Ar atmosphere with the sintering-aid gas, almost the same microstructural features were observed in the SEM micrograph as that of the sample sintered in the same atmosphere using dense compacts (Fig. 6(a)), excluding that the grain sizes of both B_4C and secondary phases were larger. The EDS spectrum for the pocket phase with irregular shape showed a strong Si peak (Fig. 6(b)). Thus, the presence of SiC was confirmed by the SEM-EDS analysis, whereas the Al compounds identified by XRD were not found on the polished and etched surfaces of the samples. In order to find the Al compounds, polished surfaces of the sample were observed without etching (Fig. 7(a)), since those compounds might be removed during the etching procedure. Fig. 7(b) shows the result of spot EDS analysis on the upper bright grain. Both Al and Si peaks in the spectrum suggested that the phase was the Al–Si compound. By contrast, only strong Al peak was detected for the lower bright grain next to the large pore (Fig. 7(c)). It is likely that the grain was Al_4C_3 which was identified by the XRD analysis. The surfaces of both grains were uneven, indicating that both grains were softer than B_4C and SiC and unstable in the atmosphere containing humidity. Iseki et al. reported that the hardness of the sintered Al_4C_3 was 12 GPa and that the compound possessed high reactivity with water,[11] which supports our observation. Fig. 7(d) shows the spectrum for the laminar grain at the middle of the picture. The strong carbon peak in the figure suggested that the grain was graphite. Fig. 6(a) also shows that some of the B_4C grains grew up to 20–60 μm just like the sintered sample using the dense

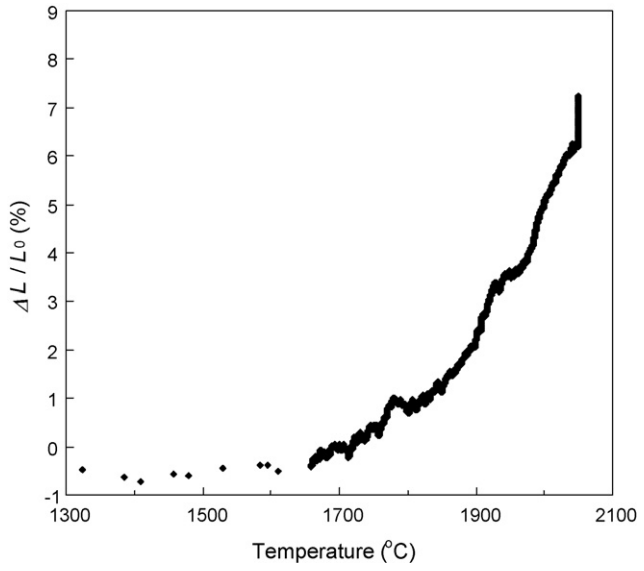

Fig. 8. Shrinkage behavior of the B_4C compact (CIPed at 490 MPa) in an Ar atmosphere with metallic gaseous species at the constant heating rate of 6 °C/min.

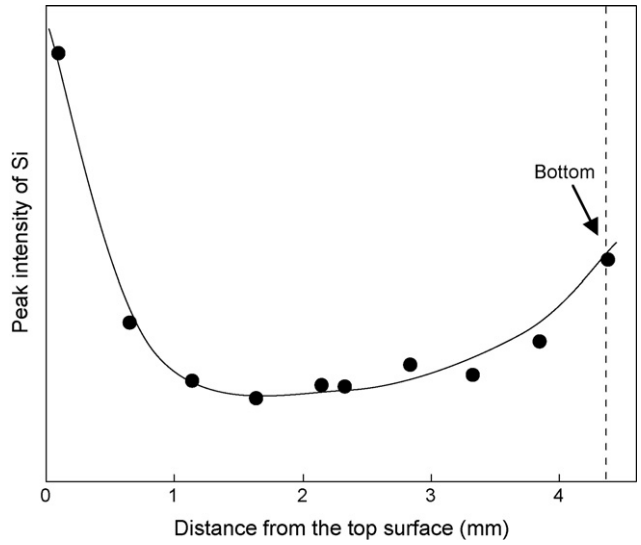

Fig. 9. Variation of the peak intensity of Si in the EDS spectrum along the downward direction of the sample sintered at 2187 °C in the Ar atmosphere with Al and Si gaseous species (CIPed at 490 MPa), which were measured on the surfaces grinded by step-by-step manner from both sides to the center. The height of the sample was about 4.3 mm.

compact (Fig. 5(a)). It should be noted that the smaller grains whose sizes were less than ~10 μm were seldom found in the figure, which was characteristic of this sample. Although the analyses of B_4C grain size were not quantitative, the apparent difference in the grain size distributions may be attributed to the amount of the liquid phase formed during the sintering.

Dilatometric measurements under a constant heating rate up to 2050 °C were conducted to elucidate the sintering mechanism of B_4C. The shrinkages of the sample heated in the Ar atmosphere containing Al and Si gaseous species were plotted against the temperature in Fig. 8. The sample started to shrink at around 1700 °C and the slope increased gradually with increasing the temperature.

4. Discussion

The increased concentrations of both Al and Si elements in the samples heated with the mixed powder of Al and SiC indicated that those elements were transported into the compacts through vapor-phase route, which were supported by the marked presence of the two elements in the sample using the loose compacts since the larger porosity of the green compacts is likely to assist the gaseous species to infiltrate into the compact easier. In order to check the mechanism, the variation of the concentration of Si impurity was evaluated at different depth of the densified body. EDS spectrums were measured on the center areas of both top and bottom surfaces of the sample heated at 2187 °C in the Ar atmosphere with gaseous Al and Si species. The size of scanned area was 620 μm × 460 μm. Both sides of sample were removed by grinding in stepwise manner (the amount of removal was about 0.5 mm for each grinding), followed by the measurements of EDS spectrums at each level of the depth. Fig. 9 shows the peak intensity of Si as a function of the distance from the top surface. The figure clearly demonstrates that the concentrations of Si at the rim parts were higher than those in the center of the sample, which was also the evidence of the vapor-phase transport for the Si element. The higher concentration of Si at the top than that at the bottom can be explained by the fact that gas infiltrated directly into the compact from the top surface while it must penetrate the porous carbon block to reach the bottom of the compact.

It was supposed that the gaseous Al species came directly form the aluminum powder in the crucible since the vapor pressure of Al is ~1 kPa at 1700 °C.[12] By contrast, gaseous Si species were not likely to be derived directly from the silicon carbide powder since the sublimation temperature of SiC is more than 2000 °C. However, it was reported that SiC was decomposed into silicon by the following reaction.[13]

$$3SiC(s) + 4Al(l) \rightarrow Al_4C_3(s) + 3Si(s) \quad (1)$$

According to Iseki et al., the reaction started at 660 °C, which is the melting point of aluminum. Enough amount of silicon ought to be supplied by the reaction during the sintering at high temperature. It is reasonable to expect that some amount of gaseous Si species were formed already at the temperature of 1700 °C at which the shrinkage of the compact started since the vapor pressure of silicon is ~10 Pa at 1700 °C.[12]

Inomata et al. reported that both Al_4SiC_4 and $Al_8B_4C_7$ could be synthesized in the ternary system of SiC–Al_4C_3–B_4C at 1800 °C.[14] They also found that plenty amount of liquid phase was formed in the compositional region vicinity to the $Al_8B_4C_7$ phase at this temperature. It is likely that the liquid phase was generated in our case when the compacts were heated in the sintering-aid gases since SiC, Al_4C_3 and Al_4SiC_4 phases were identified in the densified B_4C sample. The irregular-shaped SiC grains in Figs. 5(a) and 6(a) are supposed to be precipitated from the melt, since SiC never melts but sublimates. The fact that the starting temperature of shrinkage was ~1700 °C also implied the formation of liquid phase in the ternary system for our densified samples. Therefore it is reasonable to deduce that the formation of liquid phase might promote the densification of B_4C under ambient pressure.

It is easy to expect that many new important applications of B_4C ceramics will be developed through the pressureless sintering method since the technique enable to produce large and complex-shape components with much less machining cost, say, about one third of those for the conventional hot-pressing route. The potential applications to such products would be categorized into two groups depending on the merits of the B_4C. The first group of the products would be those which take an advantage of its highest specific elastic modulus among the practical ceramics, such as the components where both high accuracy in positioning and speed in motion is required. For example, elements used in the robot arm and stepper in the semiconductor devices, etc. The aerospace industries would also adopt the B_4C ceramics as the constitutive components because of the necessity of lightweight materials. The other group of the products would be consisted of the items which make use of its very high hardness, such as the components with resistance to wear in sev-

erer circumstances is needed. The representative applications are sand blast nozzles and cutting tools. Thus, the pressureless sintering route of B_4C promises wide applications in an inexpensive way.

5. Conclusions

Boron carbide was successfully densified up to 97.4% of the theoretical without external pressure at a temperature of 2226 °C when the compacts were heated in the Ar atmosphere containing gaseous Al and Si species. Impurities and crystalline phases in the densified samples were assessed by X-ray fluorescence and XRD analyses. Microstructural observations with SEM and EDS were performed to locate the secondary phases detected in the XRD analysis. Dilatometric measurements during heating the compact in the sintering aids gas at a constant rate of 6 °C/min were also conducted to estimate the shrinkage-starting temperature. The following results were obtained.

1. SiC, Al_4C_3 and Al_4SiC_4 were formed during the sintering as the results of the reaction of B_4C with gaseous Al and Si species which were derived from the powder mixture of Al and SiC in the same graphite crucible.
2. The secondary phases were found in the irregular-shaped pockets for the densified samples. The densification of the compacts started around the liquid-formation temperature for the system reported in the literature. The results implied that the formation of the liquid phase might play a great role in the densification process.
3. A variety of B_4C components are expected to be developed since complex-shaped products can now be available with lower cost than the conventional ones.

References

1. Thevenot F. Boron carbide—a comprehensive review. *J Eur Ceram* 1990;**6**:205–25.
2. Suzuki H, Hase H, Maruyama T. Effect of carbon on sintering of boron carbide. *J Ceram Soc Jpn* 1979;**87**(8):430–3.
3. Schwetz KA, Grellner W. The influence of carbon on the microstructure and mechanical properties of sintered boron carbide. *J Less-Common Met* 1981;**82**:37–47.
4. Dole SL, Prochazka S, Doremus RH. Microstructural coarsening during sintering of boron carbide. *J Am Ceram Soc* 1989;**72**(6):958–66.
5. Lee CH, Kim CH. Pressureless sintering and related reaction phenomena of Al_2O_3-doped B_4C. *J Mater Sci* 1992;**27**:6335–40.
6. Sigl LS. Processing and mechanical properties of boron carbide sintered with TiC. *J Eur Ceram* 1998;**18**:1521–9.
7. Kim DK, Kim CH. Pressureless sintering and microstructural development of B_4C-TiB_2 composites. *Adv Ceram Mater* 1988;**3**(1):52–5.
8. Lee H, Speyer RF, Hackenberger WS. Sintering of boron carbide heat-treated with hydrogen. *J Am Ceram Soc* 2002;**85**(8):2131–3.
9. Lee H, Speyer RF. Pressureless sintering of boron carbide. *J Am Ceram Soc* 2003;**86**(9):1468–73.
10. Kumazawa T, Honda T, Zhou Y, Miyazaki H, Hyuga H, Yoshizawa Y. Pressureless sintering of boron carbide ceramics. *J Ceram Soc Jpn* 2008;**116**(12):1319–21.
11. Iseki T, Kameda T, Maruyama T. Some properties of sintered Al_4C_3. *J Mater Sci Lett* 1983;**2**:675–6.
12. ULVAC Inc. *Vacuum Handbook*. Tokyo: Ohmsha Ltd.; 2002. pp. 159–162.
13. Iseki T, Kameda T, Maruyama T. Interfacial reactions between SiC and aluminum during joining. *J Mater Sci* 1984;**19**:1692–8.
14. Inomata Y, Tanaka H, Inoue Z, Kawabata H. Phase relation in SiC-Al_4C_3-B_4C system at 1800 °C. *J Ceram Soc Jpn* 1980;**88**(6):353–5.